Title	Physical and numerical analysis of a concept offshore wind farm service vessel hull design
Authors	Shanley, Matthew;Murphy, Jimmy
Publication date	2014
Original Citation	Shanley, M. and Murphy, J. (2014) 'Physical and numerical analysis of a concept offshore wind farm service vessel hull design', Design & Operation of Wind Farm Support Vessels 2014 Proceedings, The Royal Institution of Naval Architects, London, UK 29-30 January, pp. 155-163.
Type of publication	Conference item
Link to publisher's version	https://www.rina.org.uk/windfarm-vessels.html
Rights	© 2014: The Royal Institution of Naval Architects
Download date	2024-04-20 15:35:10
Item downloaded from	https://hdl.handle.net/10468/7343

PHYSICAL AND NUMERICAL ANALYSIS OF A CONCEPT OFFSHORE WIND FARM SERVICE VESSEL HULL DESIGN

M Shanley and J Murphy, Beaufort Research, University College Cork, Ireland

SUMMARY

Wind turbine maintenance and access during high sea states is a key issue for the successful operation of an offshore wind farm. Currently there is a 1.5m significant wave height (Hs) limit for the standard 'step over' method of transferring personnel to an offshore wind turbine. Increasing the Hs that offshore wind turbines can be accessed at would reduce the lifetime, levelised cost of energy and address a health and safety issue.

The paper addresses this issue by examining a concept hull design for an offshore wind farm service vessel. The proposed design reduces the vessel's heave and motion by dampening its response to the wave motion. The design underwent both numerical and physical methods of testing. The numerical modelling was carried out in a 3-D wave basin built in ANSYS CFX and is based on symmetry across the hull which allows for three degrees of freedom. Physical modelling at 1:25 scale took place in the wave basin at Beaufort Research in University College Cork. A number of variations of the concept were tested and the results showed the aspects of the concept that could be beneficial to personnel transfer, through reduced response amplitude operators at zero forward speed.

NOMENCLATURE

A_f	Flap stroke length at top of domain (m)
A_1	Area under the GZ curve (m deg)
A_{wl}	Area at waterline (m^2)
D	CFX Domain Height (m)
F	Force component (N)
g	Gravitational (m s^{-2})
$\overline{GM}$	Metacentric height (m)
H	Wave height (m)
h	Still water height (m)
h_e	Specific enthalpy (m^2 s^{-2})
h_{tot}	Total enthalpy (m^2 s^{-2})
I	Moment of inertia (m^4)
I_a	Moment of added inertia (m^4)
K	Thermal conductivity (kg m s^{-3} °K^{-1})
k	Wavenumber (m^{-1})
M	Mass (kg)
M_a	Added mass (kg)
p	Pressure (N m^2)
T	Temperature (°K)
T_P	Natural Period of Pitch (s)
T_R	Natural Period of Roll (s)
T_H	Natural Period of Heave (s)
t	Time (s)
U	Vector of velocity $U_{x,y,z}$ (m s^{-1})
u	Velocity component (m s^{-1})
$\overline{V}$	Displaced volume (m^3)
S_E	Energy source (kg m^{-1} s^{-3})
S_M	Momentum Source (kg m^{-2} s^{-2})
S_0	Stroke Length (m)
S_h	Horizontal spacing (m)
S_v	Vertical spacing (m)
X_{disp}	Flap displacement at height z (m)
z	Distance from still water level (m)
γ	Dynamic viscosity (kg m^{-1} s^{-1})
θ	Roll angle (deg)
λ	Wavelength (m)
μ	Molecular viscosity (kg m^{-1} s^{-1})
ρ	Density (kg m^{-3})
τ	Stress tensor (kg m^{-1} s^{-2})
ω	Angular frequency (rad s^{-1})

1.   INTRODUCTION

The vessels utilised when accessing offshore wind turbines, must keep their motion minimised in order to operate safely. The wave-induced accelerations on the vessels hinder the transfer of personnel from vessel to wind turbine as well as the operation of a crane for the transfer of replacement parts. In addition, when operating a wind farm it is extremely costly to have wind turbines broken down and unable to produce electricity. Increasing the weather window that a vessel can get service personnel on and off the wind turbine, directly increases the wind farms output.

A program for the relative motion calculator between a wind turbine and a service vessel has been created by NTNU [1]. The primary input to the model is the vessel RAO and the prevailing wave conditions, thus a reduction in zero speed RAO would result in a decrease in the relative motion and an increase in the weather window.

The majority of displacement multihull vessels in current service are designed using the National Physics Laboratory (NPL) hull form series developed by Baily in 1976 [2]. Offshore wind farm service providers have developed these designs to create vessels particularly suited for offshore wind farm maintenance. This is by manipulating the bow and stern hull form and even using deep-V hull forms. These modifications have provided improvements, however to access wind turbines in seastates with a Hs of 3m or more, radically new designs must be considered [3, 4].
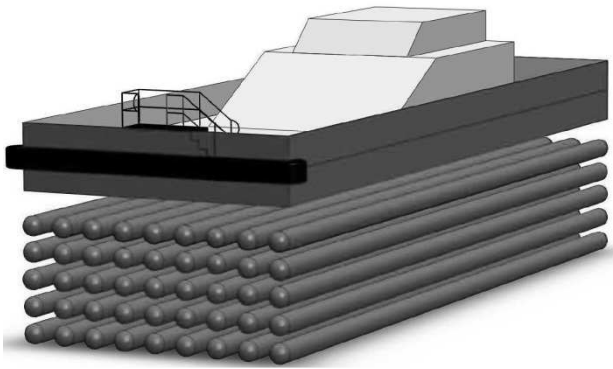
Figure 1: Concept Model Design

This paper proposes a novel new design. The concept is to have a hull composed of a number of buoyant tubes. The buoyant tubes dampen the vessel's motions, due to the viscous action of the water around the tubes. See Figure 1 for an image of the concept design.

2. INITIAL TESTING

Initially, physical testing was carried out on the model concept to investigate the possible potential of the concept design. A 1/50th scale model of an offshore supply vessel (LOA 80m, beam 20m displacing 3000tons) was tested, and a monohull vessel of the same size was also tested for comparison [5].

The Authors concluded from the initial physical testing that the design had merit. The RAOs were significantly reduced in the 6 - 12 second range, which encompass the normal operating conditions of the North Sea. Based on the physical testing, static stability calculations, regulations and standards, a refined design for a wind farm service vessel was determined. This design is discussed in the current paper.

3. REGULATIONS, RULES AND STANDARDS

The vessel is intended to be wind farm service provider category 1 as outlined by the Det Norske Veritas, (DNV) regulations. These requirements limit the vessel to a length of 24m and, the maximum number of passengers to 12 [6].

In July of this year, 2013, DNV updated their rules for classification of ships 'Offshore Service Vessels, Tugs and Special Ships', in part 5, chapter 7, section 23 they detail the requirements of vessels for windfarm maintenance. For the standard step over transfer system, the limits are expressed through wind wave and, current forces balanced with thruster forces [7]. Hence, according to the standard, increasing the thruster force, increases the weather window of personnel transfer. The effect of the vessel's RAO on the safety of transfer is thus negated. However, the vessel must operate close to the wind turbine and this study focused on vessel RAO.

The static stability of the craft can be analysed under the category of a multihull craft in Annex 7 of the 2000 HSC Code [8]. In particular the area under the GZ curve (A_1) should be at least;

$$A_1 = 0.055 \times 30°/\theta \qquad (1)$$

Where θ is in this case the angle of deck immersion.

4. MODEL DESIGN

In this study, the vessel was designed as a wind farm service provider category 1, as outlined by the Det Norske Veritas, (DNV) regulations [6,7].

On average, a wind farm service vessel has a beam of 8m and a displacement of 65 tonnes. Hence, the concept design was analysed with these parameters fixed. A design that met the above requirements and was statically stable which also adhered to the fundamental design concept, resulted in a design with the following parameters as illustrated in Figure 2:

- Horizontal spacing (S_h) 1.259m
- Vertical spacing (S_v) 0.9m - 1.8m
- External radius of tubes 0.225m
- The top of the deck is 2.938m above the waterline
- Draft is 1.987m
- Roll angle at deck immersion is 23°

The designed total mass of the vessel as stated earlier is to be 65 tonnes. At this early design stage, this was broken down into three components: Firstly, the buoyant tubes and associated supporting structure at 39 tonnes, secondly the deck structure at 15 tonnes and thirdly a cargo of 11 tonnes.
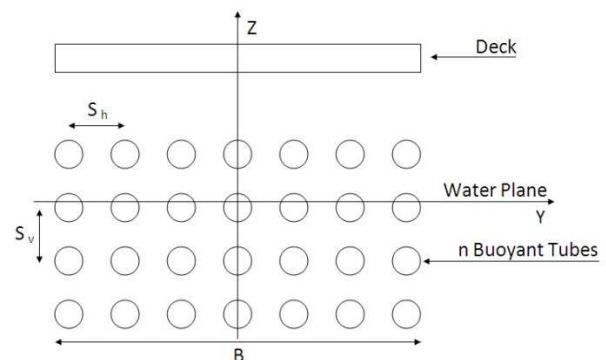

Figure 2: Beam view showing the different variables

4.1 STATIC STABILITY

The stability curve (GZ) presented in Figure 3 while meeting the requirements of the HSC code [8] has a sharp dip at an angle of 10 degrees roll. This did not present a problem in testing as sea keeping was not examined, however in models 5000 and 6000, stabilisers were incorporated to increase the waterplane area and

hence the static stability of the model, as they tended to roll easily.

The static stability of the vessel is similar to that of a SWATH vessel in that, it can vary significantly with roll, and pitch angle, causing uncertain movement.

From the GZ curve presented in Figure 3 the area under the curve is 0.1113 m.rad, which is greater than 0.07122 m.rad from equation 1. The HSC Code also states, 'The maximum GZ value shall occur at an angle of at least $10°$' that it clearly does as it is still increasing at $23°$.
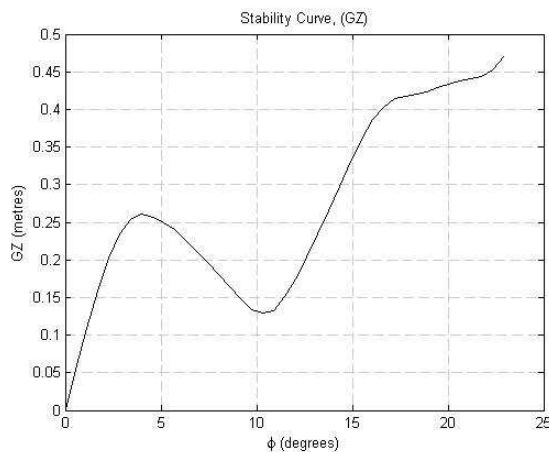

Figure 3: Stability Curve for Model 1000

However, the GZ curve rises and falls as the geometry of the water plane area changes with the vessel's roll angle, Figure 3. The effect of this, means that the vessel becomes increasingly more unstable as roll angle increases, and would have a tendency to loll at an ungainly angle. When this prevented the vessel from righting itself in the seastates tested, stabilising options were employed.

The metacentric height is considerably larger than most vessels in the North Sea and so the vessel's roll period will likely fall outside the spectral range of periods for North Sea conditions. The longitudinal metacentric height GML was 52.6 m.

5. PHYSICAL MODEL TESTING

5.1 SETUP

A 1:25 scale physical model testing of the vessel was carried out in the Beaufort-HMRC's wave basin in both regular and irregular wave simulations. In addition, the model was placed behind a scale model of a wind turbine to determine the effect it would have on the vessel's motions. The natural periods of the vessel in Heave, Pitch, and Roll were also determined.

The model was constructed primarily from 4mm polycarbonate, balsa wood coated with Original Yacht Varnish, 4mm stainless steel bolts and lead ballast. The model was slack moored to maintain position and avoid additional forces being imparted on the model.

To thoroughly test the concept, a number of variations on the theme were tested. To achieve this, the vertical spacing (S_v) of the model was varied, see Figure 2, a heave plate was also added. This resulted in ten configurations of the design to be tested shown in Figure 5 without heave plates. Due to the change in geometry of the model, the metacentric height, draft and centre of gravity varied with each model configuration to maintain static stability.
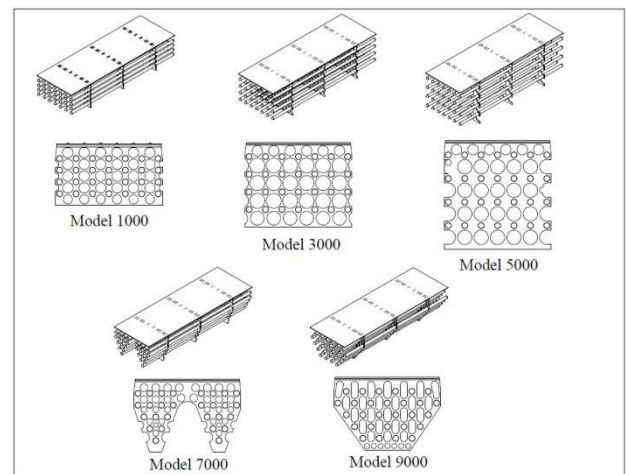

Figure 4: Model Configurations

Test ID	Description
1000	0.9m S_v spacing without a heave plate
2000	0.9m S_v spacing with a heave plate
3000	1.5m S_v spacing without a heave Plate
4000	1.5m S_v spacing with heave plate
5000	1.8m S_v spacing no heave plate
6000	1.8m S_v spacing with a heave plate
7000	Catamaran style without a heave plate
8000	Catamaran style with a heave plate
9000	Monohull style without a heave plate
10000	Monohull style with a heave plate
11000	Model 6000 placed behind a monopile

Figure 5: Test Description

Model	Mass (kg)	Draft (m)	COG (m)	GM (m)
1000	64863	2	2.75	5
2000	74473	2.675	2.4	3.8
3000	64863	2.95	2.55	6.1
4000	87926	4.3	2.625	3
5000	74072	3.875	2.725	4.9
6000	101699	5.65	3.95	3.6
7000	64863	2.975	3.65	6.5
8000	72070	3.65	3.075	7.2
9000	64863	2.85	3.425	5.2
10000	66993	3.6	2.675	5.4

Figure 6: Model details (Presented at Prototype Scale)

5.2   NATURAL PERIOD

The natural period of roll, pitch and heave of a vessel are dependent on the geometry and mass variables of the vessel as well as the added mass component, as shown inn equations 2 & 3. The added mass for unusual, complex geometries are difficult to predict and rely on empirical methods to estimate.

The equation for Roll and Pitch

$$T_{R,P} = 2\pi \sqrt{\frac{I+I_a}{\rho g \overline{V}.\overline{GM}}} \qquad (2)$$

Where I and I_a are the inertia and the added inertia of rotational motion, i.e., roll and pitch.

Equation for heave is:

$$T_H = 2\pi \sqrt{\frac{M+M_a}{\rho g \overline{V}.A_{wl}}} \qquad (3)$$

Where M and M_a are the mass and the added mass of the vessel.

The still water approach for decay periods was carried out with each of the model configurations tested. The vessel was inclined to an initial heel and then released. The results are presented at prototype scale in Figure 7 below.

Model	Pitch (s)	Heave (s)	Roll (s)
1000	2.2	2.1	3.6
2000	3.7	7.9	3.4
3000	2.1	2.2	3.9
4000	6.7	7.2	5.9
5000	2.5	2.2	4.5
6000	6.7	7.2	6.6
7000	3.2	2.1	3.3
8000	6.0	6.4	4.9
9000	2.4	2.4	3.4
10000	6.6	7.0	6.1

Figure 7: Natural Periods (Presented at Prototype Scale)

The biggest effect on natural period was the addition of the heave plate. When separated it can be seen that;

- The natural pitch period without a heave plate is between 2.1s and 3.2s or 0.3Hz and 0.5Hz. With a heave plate this becomes 6.0s to 6.7s or 0.15Hz to 0.17Hz.
- The natural heave period without a heave plate is between 2.1s and 2.4s or 0.4Hz and 0.5Hz. With a heave plate this becomes 6.4s to 7.2s or 0.14Hz to 0.16Hz.
- The natural roll period without a heave plate is be- tween 3.3s and 4.5s or 0.2Hz and 0.3Hz. With a heave plate this becomes 5.0s to 6.6s or 0.15Hz to 0.2Hz.

The natural periods without a heave plate placed the model's natural frequencies outside the frequency range of the North Sea, but when the heave period was added the natural frequencies were inside the range tested, however there is no indication that this is the case within the RAO results in section 5.3.

5.3 FACILITIES

The Physical model testing was carried out in the Beaufort-HMRC wave basin. The basin is 25m long and 18m wide with a depth of 1m. The waves are generated by a forty bottom-hinged (at 0.7m depth) flap-type paddles with active absorption and at the opposing end of the tank, there is a wave absorbing beach.

The motions of the vessel were determined using the Qualysis ProReflex, non-contact 6 DOF, motion capture measurement system. This system enables non-contact, accurate motion measurement, using a set of reflective markers attached to the device, and a camera system to track the markers.

Wave heights were recorded with current based wave probes provided using National Instruments LabVIEW Real-Time embedded controllers.

5.4   PHYSICAL MODELLING RESULTS

The results of the physical model testing clearly demonstrate the effect of a heave plate, and draft on the vessel's motions. The vessel's RAO is reduced in both heave and pitch as the vessel's draft increases, and a dramatic reduction occurs due to the introduction of a heave plate to the designs. A graph detailing the heave and Pitch RAO for all eleven cases is shown below in Figure 8.

It can be seen that the heave RAO tends to 1 at 0.08Hz (12.5s). The heave motion is reduced by more than 50% for frequencies greater than 0.14Hz when a design with a deep draft (5.65m) and a heave plate is used. In addition the effect of the natural period of heave is not noticeable in the results.

The graph of pitch motion shows that the natural period of pitch is between 0.225Hz and 0.23Hz for all models. This is inconsistent with the decay tests, likely to be due to the vessel's tubular hull structure. The designs tested, show again the benefit of using a heave plate and designs with large drafts as can be seen with the decreasing RAO curves based on draft and heave plates.

In addition, model 6000 was tested behind a monopile to simulate the effect a monopile would have on the vessel's motions at time of transfer. The results were quite similar with the heave motion being marginally lower for frequencies below 0.13Hz in heave and 0.16Hz in pitch.
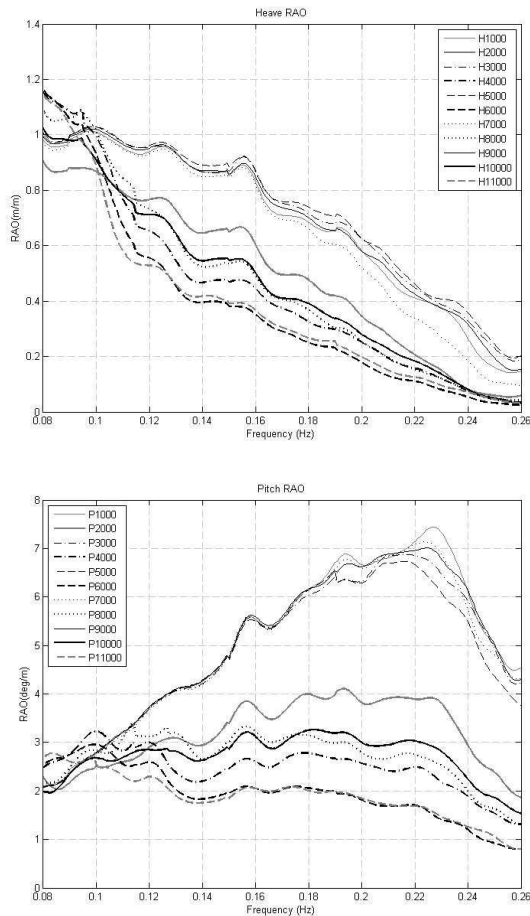

Figure 8: RAO from Physical Model Testing

6. NUMERICAL MODELLING

6.1 ANSYS CFX

Ansys CFX was used to numerically model the vessel, due to the nature of the concepts design meant that the assumptions for frequency domain analysis with potential flow theory were not valid in this case. Firstly, the water plane area of the vessel changes greatly with small angles of roll and pitch and secondly the concept sets out to use viscous effects to reduce the vessel's motions. Hence, to analyse the concept numerically, a software package that computed the vessel's movements

in the time domain and accounted for viscous flow was required. Computational fluid Dynamics (CFD) met that requirement as it computes the full Navier-Stokes equations. Specifically Ansys CFX solves the unsteady Navier-Stokes equations in their conservation form.

The Navier-Stokes Equation:

$$\frac{\partial u}{\partial t} + (u \cdot \nabla)u = -\frac{1}{\rho}\nabla p + \gamma\nabla^2 u + \frac{1}{\rho}F \qquad (4)$$

Ansys CFX was chosen as it has incorporated algorithms that can compute a free surface, and the movements of a floating body in the fluid. In addition, it is industry proven software.

CFD analysis is a time and computationally expensive exercise, but a requirement if this concept is to be adequately modelled numerically. CFX is not at a stage to replace physical model testing. It however can add to physical tests and expedite the process of optimising the design. The fluid modelling software Ansys CFX solves the unsteady three-dimensional Reynolds Averaged Navier-Stokes (RANS) Equation for simulating a 3-D numerical wave tank and floating object. The general-purpose RANS solver Ansys CFX, which is based on the Finite Volume Method (FVM), was used for the present simulation. Multiphase simulations for free surface deformation were computed using Volume of Fraction (VOF) method. The movement of the vessel was computed using the rigid body solver incorporated in Ansys CFX.

6.1 (a) Relevant Ansys CFX Theory

The Navier-Stokes equations are the fundamental equations of fluid flow and heat transfer, solved be CFX-Solver. They are partial differential equations.

The fundamental equations the CFX uses in the presented work are detailed here. The governing Transport equations for Mass, Momentum and energy conservations are detailed. The Continuity Equation is:

$$\frac{\partial \rho}{\partial t} + \nabla \cdot (\rho U) = 0 \qquad (5)$$

The momentum Equations are:

$$\frac{\partial(\rho U)}{\partial t} + \nabla \cdot (\rho U \otimes U) = -\nabla p + \nabla \cdot \tau + S_{\mathrm{M}} \qquad (6)$$

Where, U vector of velocity $U_{x,y,z}$, p is the static pressure, S_{M} represents external momentum sources and τ is the stress tensor, related to the strain by:

$$\tau = \mu\left[\nabla U + (\nabla.U)^{\mathrm{T}} - \frac{2}{3}\delta\nabla \cdot U\right] \qquad (7)$$

Where, μ is the molecular viscosity.

The Total Energy equation in CFX is:

$$\frac{\partial(\rho h_{\text{tot}})}{\partial t} - \frac{\partial p}{\partial t} + \nabla \cdot (\rho U h_{\text{tot}}) = \nabla \cdot (K \nabla T) + \nabla \cdot (U \cdot \tau) + U \cdot S_M + S_E \quad (8)$$

Where h_{tot} is the total enthalpy, related to the static enthalpy $h(T,p)$ by:

$$h_{\text{tot}} = h_e + \frac{1}{2} U^2 \quad (9)$$

Where the term $\nabla \cdot (U \cdot \tau)$ represents the work due to viscous stresses and is called the viscous work term and the term $U \cdot S_M$ represents the work due to external momentum sources and is currently neglected by CFX.

Multiphase simulations for free surface deformation were computed using Volume of Fraction (VOF) method. The movement of the vessel was computed using the rigid body solver incorporated in Ansys CFX.

The VOF Method that Ansys CFX uses is the Volume fraction of the qth fluid, α_q. Each cell in the domain is assigned its own specific variables and the continuity equation is solved for the volume fraction of the phases. For the qth phase:

$$\frac{d}{dt} \alpha q + u. \nabla \alpha q = 0 \quad (10)$$

$$\sum_{q=1}^{n} \alpha q = 1 \quad (11)$$

The momentum equation is solved throughout the domain, and the resulting velocity field is shared among the phases. The momentum equation depends on the volume fraction of all phases through the fluid properties.

$$\rho = \sum_{q=1}^{n} \alpha q. \rho q \quad (12)$$

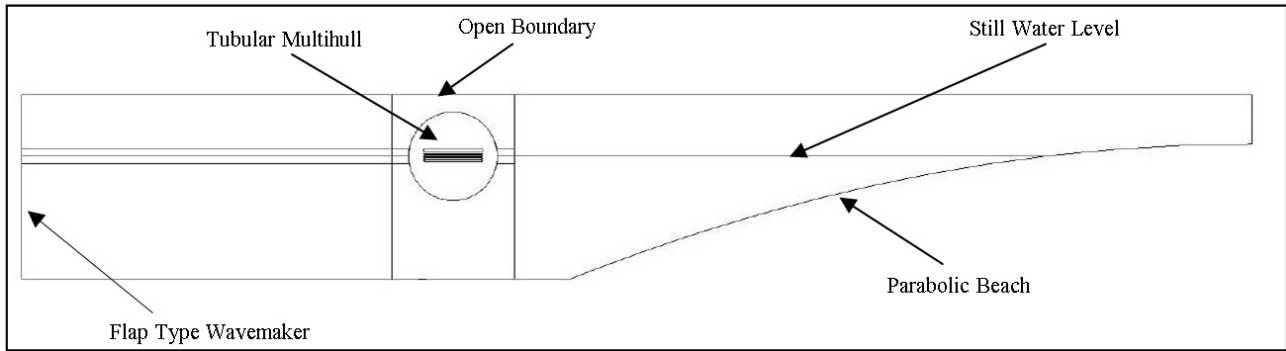Further (more detailed) information can be found in the Ansys CFX documentation. [9, 10]

Figure 9: CFD Layout

6.2   CFD SETUP

6.2 (a)   Boundary Conditions

Figure 9, above shows the domain setup, there is a flap type wave-maker on the left that generates waves according to the following formula [12].

$$\frac{H}{S_0} = \frac{4 \sin kh}{\sinh 2kh + 2kh} \left[\sinh kh + \frac{1 - \cosh kh}{kh} \right] \quad (13)$$

Where: $k = \frac{2\pi}{\lambda}$ and h is the height of water and λ is the wavelength.

The following equation 14, was used to control the mesh motion at the flap wave-maker [11]:

$$X_{\text{disp}} = \frac{z+h}{D} A_f. \sin \omega t \quad (14)$$

There is an opening boundary at the top, which allows air to enter and exit as required as the waves oscillate. There is a parabolic beach at the end of the wave tank to dissipate the wave energy by means of wave breaking. A parabolic beach was found to be most effective at this, whilst keeping the domain size to a minimum. This is a full scale simulation with a domain of 500m long, 75m

high and a water depth of 50m. The model allows 150m for the waves to fully form and allow for the initial exponential decay. There is then a 50m section to place the model in. The model is shown in Figure 9 inside a circle. The circle and other lines shown inside the domain are fluid to fluid boundaries to aid mesh optimisation [10, 12].

Symmetry was utilised in the model to keep the mesh size to a minimum, for a three dimensional simulation. The thickness of the entire domain is 1/14 of the vessel width. This results in a half cylinder and half the spacing between cylinders, with an overall domain thickness of 0.5 x Sh = 629.5mm

The front and rear faces of the simulation have a symmetry boundary condition, also the vessel's movements are restrained to 3 degrees of freedom, Heave, Pitch and Surge.

6.2 (b)   Mesh and Timestep

To achieve a convergent solution a domain that had 2,028,443 mesh elements was required. The mesh was refined at the water surface, to prevent what is known as 'numerical damping' where the wave height diminishes

as it propagates. This numerical damping is effected by the timestep also and it is recommended that the timestep be 1/100 of the wave period [13]. In the simulation presented, a timestep of 0.05s was used.

Mesh and timestep sensitivity analysis were carried out both on the calibration model and on the rigid body model. Due to the nature of the flow around the tubes and the forces induced on them, the coupling between the rigid body solver and the fluid solution was enhanced to achieve a convergent solution. Relaxation of the mesh motion was also required.

To determine the accuracy of wave propagation throughout the tank, a series of simulations were run without the rigid body in the domain.

6.3   CFD RESULTS

In Figure 10, the RAO results from the CFD analysis in in Ansys CFX are shown alongside the regular RAO results from the physical model tank testing (model 1000). Close similarity is displayed at the lower frequency ranges. However, at higher frequency ranges poorer similarity is displayed.

The CFD model was constructed prior to any physical modelling results and hence no inputs from the physical model to achieve the correlation. This shows that a CFD numerical wave tank is a powerful tool in accurately modelling unusual shapes. This result is a validation of the CFD method of testing novel hull forms.
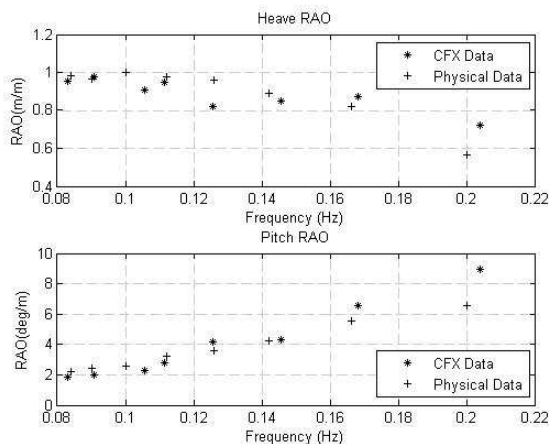

Figure 10: Model 1000 Regular RAO from Physical Model Testing compared with results from Ansys CFX

7.   **COMPARISON WITH OTHER PUB-LISHED DATA**

The concept hull design analysed in this paper is different from those considered in other studies, hence a direct assessment cannot be made. However, some comparisons with other vessel's of a similar size can be made to appreciate the general trends of the results.

Though published in 1975, a report by the U.S. Naval Ship and Development Centre regarding the seakeeping of naval ships provides relevant data for comparison [14]. They present full scale results for a 25.9m (85-foot) hard chine boat who they said 'represents a workboat whose response characteristics as a Navy workboat are already known.' Table 4 in the report outlines the RMS responses of the ship. When converted to metres it shows that the vessel's heave RAO at 6 seconds is 0.6 , at 8 seconds 0.8 , at 10 seconds 0.9 , and at 14 seconds the RAO is 1.0. The pitch RAO is at 6 seconds 6.0, at 8 seconds 5.0, at 10 seconds 3.9, ad at 14 seconds 2.2. This shows that the design presented in this paper has a reduced pitch overall and that, the heave RAO is better with the heave plate than the monohull but worse if the heave plate is not included. It should be noted that, the RAO used in the comparison is from Table 4 of the navel report[14] subsequently converted to metres and that the results presented in the report in Figure 8a [14] show that the RAO's are half that discussed above. The author has concluded that there is a mistake here as it is quite unreasonable that a 25.9m hard chine monohull without bilge keels would have a heave RAO of 0.5 in waves with a 14s period.

The results from [15] present the model tests of a 43m catamaran hull. The RAOs were presented in a non-dimensional frequency format, converting to the style presented in this paper a comparison can be made. The heave RAO followed a trend line close to the designs tested with a heave plate presented in this paper. The pitch RAO is very low compared to the designs presented here and that is probably due to the length of the vessel [15].

In the results published in [16, 17] numerical and physical modelling testing of a high-speed catamaran at zero forward speed are presented. The results show that the 64m V-1 catamaran significantly outperformed the designs presented in this paper [16, 17].

8.   **CONCLUSIONS**

The physical model testing showed little improvement over a conventional vessel of the same size. Especially when accounting for the difficulties in seakeeping, and fuel economy the design would create.

The results do conclusively show that, the deeper the draft of the vessel, the better the RAO and the addition of a heave plate made a marked improvement.

An important conclusion from the testing carried out in this paper was that the numerical model showed close agreement with the scaled physical model. This showed the dependability of CFD wave tank modelling. The validation of this method of testing is a significant conclusion from the work undertaken. This illustrates that a CFD numerical wave tank is a powerful tool in accurately modelling unusual shapes. This result is a

validation of the CFD method of testing novel hull forms. It should be noted that there were no inputs from the physical model to achieve the correlation.

There will be a market for an improved offshore wind maintenance vessel, due to the increase in maintenance required for the UK's upcoming round three projects. Therefore, a design for such a vessel based on the existing codes and static stability calculations is warranted.

9. ACKNOWLEDGEMENTS

References

1. BERG E., 'Calculation of Relative Motion Between Offshore Wind Turbine and a Service Vessel', *Norwegian University of Science and Technology*, 2012.

2. BAILY D., 'The NPL High Speed Round Bilge Displacement Hull Series', *RINA*, 1976.

3. MARSH G., 'Deep Offshore O&M: Accessing All Areas', *Renewable Energy Focus*, 2013.

4. MARSH G., 'WFSV: Hull form focus', *Renewable Energy Focus*, 2012.

5. SHANLEY M., Murphy J., and Molloy P., 'Offshore Wind Farm Service Vessel, Hull Design Optimisation', *ICOE*, Dublin, 2012.

6. D. N. V. Det Norske Veritas, 'Tentative Rules for Service Craft Carrying up to 12 Passengers', *Det Norske Veritas*, 2012.

7. D. N. V. Det Norske Veritas, 'Offshore Service Vessels, Tugs and Special Ships', *Det Norske Veritas*, 2013.

8. The Maritime and Coastguard Agency, 'International Code of Safety for High Speed Craft', *2000 HSC Code*, 2009.

9. ANSYS CFX. 'User Reference Material', *ANSYS, Inc.*, 2010.

10. LAL A., and ELANGOVAN M., 'CFD Simulation and Validation of Flap type Wave-Maker', *World Academy of Science, Engineering and Technology*, 2008.

11. DEAN R. G., and DALRYMPLE R. A., 'Water Wave Mechanics for Engineers and Scientists', *Prentice-Hall Inc., New Jersey*, 1984.

12. FINNEGAN W., and GOGGINS J., 'Numerical Simulation of Linear Water Waves and Wave-Structure Interaction', *Ocean Engineering*, 2012.

13. SILVIA M. C., VITOLA M. A., PINTO W. T., and LEVI C. A., 'Numerical Simulation of Monochromatic Wave Generated in Laboratory: Validation of a CFD Code', *Construcao Naval e Offshore, Rio de Janeiro*, 2010.

14. BAITIS A. E., MEYERS W. G., WOOLAVER D. A, and LEE C. M., 'A seakeeping Comparison Between Three Monohulls, Two Swaths, and a Column-Stabilised Catamaran Designed for the Same Mission', *National Technical Information Service U. S. Department of Commerce*, 1975.

15. SOARES G. C., and MARON M., 'Model Tests of the Motions of a Catamaran Hull in Waves', *RINA*, 1999.

16. FANG C. C., CHAN H. S., and INCECIK A., 'Investigation of Motions of Catamarans in Regular Waves – I', *Ocean Engineering*, 1994.

17. FANG C. C., CHAN H. S., and INCECIK A., 'Investigation of Motions of Catamarans in Regular Waves – II', *Ocean Engineering*, 1996.

10. AUTHORS BIOGRAPHY

Mr Matthew Shanley is a Ph.D. Candidate in Engineering at Beaufort-HMRC Research in UCC the title of his work is 'Innovative Measures for Servicing Offshore Wind Turbines' and is funded through the Graduate Research Education Programme in Engineering.

Dr Jimmy Murphy is the Head of Coastal Engineering & Offshore Wind Group at Beaufort-HMRC Research in UCC.